Figure-ground modulation in awake primate thalamus

Helen E. Jones[a,1], Ian M. Andolina[a], Stewart D. Shipp[a], Daniel L. Adams[b], Javier Cudeiro[c], Thomas E. Salt[a], and Adam M. Sillito[a]

[a]Department of Visual Neuroscience, University College London Institute of Ophthalmology, London EC1V 9EL, United Kingdom; [b]Beckman Vision Center, University of California, San Francisco, CA 94143; and [c]Department of Medicine, NEUROcom and Institute of Biomedical Research of A Coruña, Campus de Oza, University of A Coruña, s/n 15006, A Coruña, Spain

Edited by Robert H. Wurtz, National Institutes of Health, Bethesda, MD, and approved March 26, 2015 (received for review March 20, 2014)

Figure-ground discrimination refers to the perception of an object, the figure, against a nondescript background. Neural mechanisms of figure-ground detection have been associated with feedback interactions between higher centers and primary visual cortex and have been held to index the effect of global analysis on local feature encoding. Here, in recordings from visual thalamus of alert primates, we demonstrate a robust enhancement of neuronal firing when the figure, as opposed to the ground, component of a motion-defined figure-ground stimulus is located over the receptive field. In this paradigm, visual stimulation of the receptive field and its near environs is identical across both conditions, suggesting the response enhancement reflects higher integrative mechanisms. It thus appears that cortical activity generating the higher-order percept of the figure is simultaneously reentered into the lowest level that is anatomically possible (the thalamus), so that the signature of the evolving representation of the figure is imprinted on the input driving it in an iterative process.

vision | perception | feedback | lateral geniculate nucleus | figure-ground discrimination

Classically, our percept of the world and the objects in it is considered to derive from a collation of information from the sensory periphery, relayed via the sensory thalamic nuclei to the cortex, where salient features are detected and integrated across spatial and modality domains to generate our ongoing perception. Thus, in vision, the retinal input to the visual thalamus is relayed to the visual cortex, where the cortical circuitry assembles the components of the input into configurations that detect feature orientation and direction of motion. Further processing in the cortical circuitry beyond the primary visual cortex then provides the integration to reflect objects and objects distinguished from the background. In figure-ground discrimination, our visual system reconstructs objects from the diverse components of early distributed processing by grouping image elements and segregating them from the background as a figure. In this view, the neural mechanisms of figure-ground detection are linked to processes operating in primary and higher visual cortical areas (1–6), and the assumption is that relatively inviolate information from the visual thalamus provides the raw substructure essential for the veracity of these higher-level abstractions. However, another feature of the organization of sensory systems and the visual system is that the feedforward pathways are paralleled by extensive feedback pathways (7–9). Moreover, this feedback is reflected all the way back to the sensory thalamic nuclei, and in the visual system, certainly, it is very fast (7). What does this serve? It might logically be conjectured to be just gain control, but various studies suggest there may be more to it (7, 9–16). The question is, what? It would seem surprising that the signature of the higher-level cortical process is reflected in the visual thalamus, but it needs to be tested. Here, we consider the possibility that the high-level representation of the signal distinguishing a figure from ground might, because of the feedback connections, be reflected in the activity seen in neurons in the lateral geniculate nucleus (LGN) of the visual thalamus. This has neither been previously tested nor reported, to our knowledge, and if it is true, it would change how we view the mechanisms underpinning some aspects of the higher-level integration.

We have used the salient appearance of a figure defined by motion contrast, posited by neurocomputational models to depend on interactions among areas V5/MT, V2, and V1 (17, 18). These modeling approaches have proposed two complementary processes: one driven by detection of feature discontinuities establishing contour boundaries and the other a region filling-in mechanism that links the representation of the common features in the figure (1, 2, 5). These processes have previously been linked to mechanisms operating in primary and higher cortical areas and are suggested to involve feedback to amplify the neural response in the region representing the center of the figure (3, 4, 6, 19; but see ref. 20). The key to the tests in the experimental design, exploited here, and for earlier studies of cortical responses to figure-ground stimuli (3, 6, 21), is that the visual stimulation of the test receptive field (RF) and its near environs is identical across the "figure" and "ground" conditions, and that the figure condition is determined by a change remote to the LGN cell classical RF. Hence, any difference in LGN activation should be attributable to higher mechanisms integrating events over a larger spatial scale and feeding the information back down the system. This deduction is doubly warranted in our case, when the figure border is defined by motion contrast, and neural directional mechanisms in macaque monkey are generally accepted to be neither intrinsic to the retina nor LGN, but first developed in area V1 (22, 23) (although note ref. 24 and also see *Results*).

Results

The stimulus was a pattern of randomized drifting dots with the figure pop-out delineated by the opposite direction of motion

Significance

Perceptually, the visual cortical areas are considered to reconstruct objects from the diverse components of early distributed processing by grouping image elements and segregating them from the background as a figure. An assumption here is that raw, essentially unchanged information from the visual thalamus provides the basic pattern essential for the operation of these higher-level abstractions. However, here we demonstrate strong enhancement of neuronal firing to the figure component of a figure-ground stimulus in recordings from the visual thalamus of behaving primates. This suggests the signature of a higher-order percept is introduced into the thalamus in a reentrant manner via the corticofugal feedback connections and causes our visual input to confirm what we think we are seeing.

Author contributions: H.E.J. and A.M.S. designed research; H.E.J., I.M.A., and S.D.S. performed research; I.M.A. and D.L.A. contributed new reagents/analytic tools; H.E.J., I.M.A., S.D.S., J.C., and T.E.S. analyzed data; and H.E.J., S.D.S., and A.M.S. wrote the paper.

The authors declare no conflict of interest.

This article is a PNAS Direct Submission.

Data deposition: The research materials supporting this publication can be accessed from zenodo.org/record/11080 or by contacting either hjones@ioores.co.uk or a.sillito@ioores.co.uk.

See Commentary on page 6784.

[1]To whom correspondence should be addressed. Email: hjones@ioores.co.uk.

This article contains supporting information online at www.pnas.org/lookup/suppl/doi:10.1073/pnas.1405162112/-/DCSupplemental.

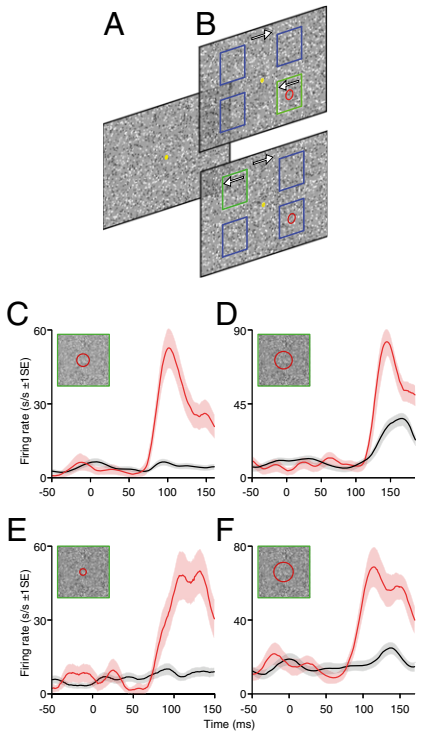

Fig. 1. Enhancement of neuronal firing when the figure, as opposed to the ground component of the stimulus, was located over the RF. (*A* and *B*) Schematic depiction (not to scale) of the stimulus and behavioral paradigm. The full-screen random dot display was initially static, with a central, yellow fixation spot (*A*). After a minimum fixation period of 400 ms, motion was initiated. A single square figure, delineated solely by its opposite direction of dot motion, was visible at one of four possible locations (indicated here by green/blue squares) either centered over the RF (depicted by the red circle), as shown in the upper panel or at an alternative location as shown in the lower panel (*B*). Monkeys were rewarded for making a saccade (within 500 ms of motion onset) to the center of the figure target. (*C–F*) Responses of four example LGN neurons. Spike density functions (SDF) to ground (black) and figure (red) stimulus conditions (±1 SE). Inset schematics show the size of the RF relative to the figure size. Time epoch commences 50ms before stimulus motion onset and ends before saccade initiation. See also Fig. S1.

of the dots within the figure and the ground (Fig. 1 *A* and *B* and *Materials and Methods*). Two macaque monkeys were trained to fixate centrally within a large 30° static random dot field. After a fixation period of at least 0.4 s, dot motion commenced to define a square figure at one of four pseudorandom screen locations, and the monkeys were trained to saccade to and refixate at the figure center within 500 ms of motion onset. Psychophysically, this is an exercise in exogenous ("bottom-up") attentional capture (25), for the monkeys had no cue and no means of predicting the figure location, which was equally frequent across the four sites.

Our results are based on recordings from 77 single-unit and 63 multiunit recordings. As similar response patterns were observed for both unit types, data for both are pooled. Our single-unit population sample largely comprised parvocellular cells, although we also obtained some recordings from koniocellular and magnocellular cells. Across the single-unit data, similar results were observed across the three cell groups (Fig. 2), and data for all cell types were therefore pooled. The RFs of parafoveal LGN cells were located centrally within the figure region for one of these figure locations, and remote from the figure border. The standard figure size was 3–4° (3 ± 0.82° SD; n = 140) but was made smaller for fields within 5° of the fovea (although never less than 2°; *Materials and Methods*). We routinely used all pairings of rightward and leftward dot motion between figure and ground thus (as noted earlier), exposing the RF to the identical set of local features across "figure" and "ground" trials (the latter being, necessarily, three times more frequent). Many LGN cells responded weakly or not at all to the ground stimulus (Figs. 1 *C–F* and 2), although some showed a small onset transient (see Fig. S2*A* for an example). This itself was surprising because it suggests there is at most a low input to the cortex from these cells in this situation. Although it is consistent with previous work reporting the presence of strong surround suppressive effects in the LGN (11, 26–28), it may also in part reflect a failure of the small LGN cell receptive fields to distinguish between the static and moving noise patterns because of ongoing motion secondary to residual eye movements. However, this lack of response contrasted with the fact that we observed a strong, long latency (median onset latency, 90 ± 2.26 ms SE; n = 140) increase in firing rate to the figure stimulus (Figs. 1 *C–F* and 2). To quantify this enhancement, we calculated a figure-ground modulation index value (FGM) for each cell by taking the difference between the averaged responses to the figure and ground conditions normalized with respect to the sum of the averaged responses to the figure and ground (*Materials and Methods*). We adopted the same analysis strategies previously used in V1 (29) (where neurons commonly exhibit strongly orientation and direction selective responses) to ensure any potential confound arising from the weak

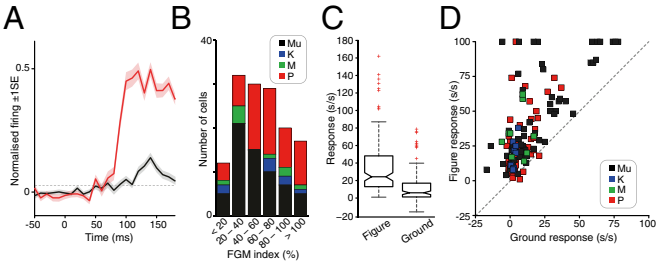

Fig. 2. Population summary data. (*A*) Averaged population responses to figure (red) and ground (black) stimulus conditions overlying the RF. Shading represents ±1 SE. Motion onset occurred at time 0 ms. Horizontal dotted line denotes background plus 99% confidence limit. See *Materials and Methods* (last paragraph) for full details of the normalization procedure. (*B*) Bar group-histogram plots the distribution of FGM (in percent) across our sample for multiunits (Mu, black), Parvocellular (P, red), Magnocellular (M, green), and koniocellular (K, blue) cells. The median FGM was 56 ± 6.07% SE; n = 140. The FGM values for each monkey were 60% (±5.69 SE; n = 91) and 45% (±12.84 SE; n = 49), respectively. There was no significant difference between the FGM values observed for the two monkeys for either the single unit data, the multiunit data, or combined single and multiunit data sets (P > 0.05 for each comparison, Wilcoxon matched pairs test). Our single unit population sample was largely comprised of parvocellular (P) cells (n = 60), although we also obtained some recordings from both koniocellular (K; n = 8) and magnocellular (M; n = 9) cells. Across our single unit data, there was no significant difference in either the magnitude of the FGM index (P = 0.7172, Kruskal-Wallis ANOVA) or proportion of cells exhibiting the effect (P = 0.118, Freeman Halton extension of Fisher Exact Probability test) across the three cell groups. (*C*) Box-notch plots of figure (*Left*) and ground (*Right*) responses (in s/s after subtraction of background activity). The horizontal line in the middle of the box shows the median response, and the notch limits signify the 95% confidence interval around the median; box limits signify 25th and 75th percentiles of the data, and the extended whiskers show 1.5 times the interquartile range. Responses outside a range 1.5 times the width of the interquartile range from the median are shown as separate points (red crosses). The two notches do not overlap vertically; thus, the corresponding medians are different at the 5% level. (*D*) Distribution of ground responses versus figure responses [in spikes per second (s/s) after subtraction of background activity] across the cell sample. Dashed line denotes the diagonal representing equal responses to both stimuli. Negative values represent cases where responses to ground stimulation were reduced below the background firing rate (27). Color conventions as in *B*.

directional biases previously reported for some macaque LGN cells (24) were controlled for (*Materials and Methods*). There was a marked figure-ground modulation of the response across our sample (median enhancement above ground, 56 ± 6.07% SE; n = 140). We illustrate this by the average population responses (Fig. 2*A* and Fig. S3), the distribution of FGM values across our sample (Fig. 2*B*), and the comparison of responses evoked by ground versus figure stimuli (Fig. 2 *C* and *D*). Approximately 90% of cells (128 of 140) showed a FGM index of 20% or more.

Having discovered such a pronounced response to the figure center, we wondered whether the response at the border might be further enhanced, as observed in V1 [albeit with a non-identical behavioral paradigm and with a static, textural mode of figure-ground delineation (6)]; border detection is a key process in filling-in models of figural discrimination, essentially setting the topographic boundaries of a neural map filled in by the figural surface features (1, 2, 5). In a subset of cells (n = 37), we also checked the effect of displacing the figure location so that the border between the figure and ground components of the stimulus was located over the RF, interlacing figure, border, and ground trials in a pseudorandom sequence, as before. There was, however, no significant difference in either the magnitude or onset latency of the responses evoked by figure and border location stimuli (P = 0.379 and P = 0.795, respectively, Wilcoxon matched pairs test; n = 37; Fig. 3). There were actually two distinct borders in our stimulus configuration, where the opposite directions of dot motion were either perpendicular or parallel to the edge of the square-shaped figure; we tested both, but noted no qualitative differences and pooled the two conditions for the population average data in Fig. 3*C*.

Our data clearly demonstrate that LGN neurons show differential spiking activity for figure compared with ground stimulation conditions in a manner analogous to the figure-ground modulation previously reported for cortical stages of the visual hierarchy. However, as the task design required the monkey to saccade to the figure, an alternative interpretation could be that a component of the neuronal enhancement in our behavioral paradigm reflected presaccadic activation. To explore this, we also recorded the responses of a number of LGN neurons whose RFs were located in very close proximity to the fovea. In these cases, a figure stimulus located over the RF also encompassed the fixation window and the monkeys were rewarded simply for maintaining fixation when the figure was located over the RF. Although the monkey did not make a saccade to the figure stimulus overlying the RF, we continued to observe the strong, long latency increase in firing rate to the figure stimulus (Fig. 4) with a marked figure-ground modulation of the response across the sample (median enhancement above ground, 59 ± 8.42% SE; n = 20).

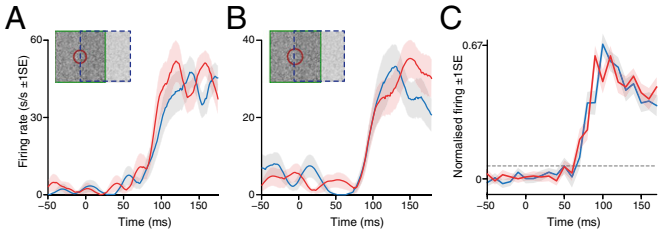

Fig. 3. Comparison of responses to figure and border stimuli located over the RF. (*A* and *B*) SDFs for two example LGN cells to conditions where the border (blue) or figure (red) was present over the RF. Conventions as in Fig. 1 *C–F*. (*C*) Population summary data plotting the averaged population responses to figure (red) and border (blue) stimulus conditions overlying the RF (n = 37). Horizontal dotted line denotes background plus 99% confidence limit. Conventions as in Fig. 2*A*.

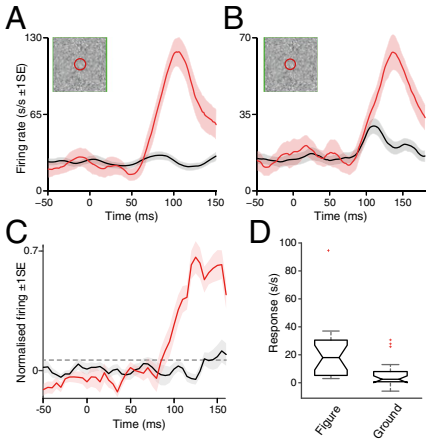

Fig. 4. Enhancement of neuronal firing to a figure located over the RF in the absence of saccades. (*A* and *B*) SDFs for two example LGN cells to ground (black) and figure (red) stimulus conditions overlying the RF. Diagrammatic conventions as in Fig. 1 *C–F*. As for our standard stimulus paradigm, the full-screen random dot display was initially static, with a central, yellow fixation spot. After a minimum fixation period of 400 ms, motion initiated and a single square figure, delineated solely by its opposite direction of dot motion, was visible at one of four possible locations. As the RFs of these cells were located very near the fovea, when the figure was centered over the RF, it encompassed the fixation window and the monkey was rewarded for maintaining fixation. When the stimulus was located at one of the three alternative locations displaced from the RF (and arranged in similar locations to those normally occupied by the nonreceptive field figure locations in our standard paradigm), monkeys were rewarded for making a saccade (within 500 ms of motion onset) to the center of the figure target as normal. (*C*) Population summary data plotting the averaged population responses to figure (red) and ground (black) stimulus conditions overlying the RF (n = 20). Horizontal dotted line denotes background plus 99% confidence limit. Conventions as in Fig. 2*A*. (*D*) Box-notch plots of figure (*Left*) and ground (*Right*) responses (in s/s after subtraction of background activity). The horizontal line in the middle of the box shows the median response and the notch limits signify the 95% confidence interval around the median; box limits signify 25th and 75th percentiles of the data, and the extended whiskers show 1.5 times the interquartile range. Responses outside a range 1.5 times the width of the interquartile range from the median are shown as separate points (red crosses). The two notches do not overlap vertically; thus, the corresponding medians are different at the 5% level.

Discussion

Our results show that the responses of LGN cells in awake behaving monkeys can be strongly modulated by a motion-defined figure-ground stimulus. In a sense, this is unexpected, given that it is generally accepted that neither contour orientation nor spatiotemporal direction of drift are explicitly represented at this level. Our results were observed with figure sizes notably larger (our standard figure sizes were 3–4°) than the LGN cells' RF diameter (0.75 ± 0.79° SD; n = 140). Thus, the figure-ground modulation we saw was for RFs that were located centrally within the figure region and remote from the figure border. This is commensurate with the results from virtually all the studies in V1 and V2 (3, 6, 21), although one study in V1 (20) only observed a modulation when the border was close to the RF. The discrepancy in this latter case has been linked to task design (3, 6, 20, 21), so it is relevant to note that our task design closely mirrored that of the former studies, rather than the latter. We believe the effect we have observed closely matches the characteristics of figure-ground modulation in the cortex and reflects the influence of feedback circuitry integrating cortical and thalamic levels. The results thus suggest that the signature of a higher-order percept is fed back into the thalamus in a reentrant manner, changing the information relayed to the cortex. This implies that this realignment of the sensory input from the thalamus, to reflect the percept initially

integrated at higher cortical levels, is an important component of the neural logic to the process extracting and testing the ever-changing features of the visual world. This new observation argues for a reevaluation of the iterative neural mechanisms that represent and extract salient features of the visual world.

A striking feature of our data is the magnitude of the modulation to the figure condition. It contrasted strongly with the minimal response shown by many of the cells to the motion of the background stimulus in isolation. We believe it is consistent with a system that relays minimal information to a "nonsalient stimulus" (7, 11) and that the "global" salience detected by higher-level feature detectors, sampling larger areas of visual space, is fed back and modulates the response to the underlying retinal excitatory input to the LGN cells by disinhibition and direct facilitation. A few cells (e.g., Fig. S2*A*) did give a transient response to the onset of stimulus motion, and these might serve to prime the cortex also, but the major point seems to be a feedback-driven "release" of excitatory drive initiated from retinotopic locations way beyond the LGN cell receptive field, with a most logical origin in MT. Feedback from MT has been shown to exert a strong influence on the earliest component of the response of V1 cells to both moving and flashing stimuli (19) and strong effects on LGN cell responses exerted from locations outside their receptive field (30).

The modulatory effect reported here greatly exceeds that observed by us or any other group for modulation of LGN cell responses by classical, extraclassical, or remote stimuli (7, 16, 31–34). It has long been acknowledged that the responses of many neurons in the visual system can be influenced by stimuli remote from the classical RF (31). A variety of effects has been reported in anesthetized animals. These effects range from nonspecific inhibitory or facilitatory effects such as "shift" or "periphery" effects predominantly linked to retinal and geniculate cell responses, to direction and orientation selective contextual effects most commonly linked to V1 and higher cortical areas such as area MT (31, 35–38). These latter, stimulus-specific contextual modulatory effects have been extensively linked to a role in local–global comparisons and in the discrimination of figure from background (29, 31, 38). A range of studies in awake behaving monkey has linked mechanisms underlying figure-ground detection to processes operating in V1 and higher cortical areas (3, 6, 21, 29). However, our study is the first, to our knowledge, to demonstrate, in awake behaving monkey, the presence of differential spiking activity for figure compared with ground stimulation conditions in the LGN that are analogous to the figure-ground modulatory effects previously demonstrated only for cortical stages of the visual hierarchy (3, 6, 21, 29). As the magnitude of the effect we observed is substantially larger than that reported for any of the previous studies of contextual modulatory effects in the LGN (7, 16, 32–34), it suggests that it draws on processes that are enhanced or only enabled in the behaving preparation.

As the speeded reaction time task design we deployed (39) required the monkey to saccade to the figure, an alternative interpretation for the differential effects we observed could be that a component of the neuronal enhancement in our behavioral paradigm reflected presaccadic activation. Although the current literature regarding perisaccadic modulatory effects in LGN would argue against the latter interpretation (40), we also obtained direct evidence against a motor-based, presaccadic interpretation by recording from cells with foveal or perifoveal fields. Robust FGM responses were still observed despite the monkey completing the task without making a saccade to the figure stimulus overlying the RF (Fig. 4), a result that directly argues against the modulation being presaccadic in origin. We have also recorded preliminary data from a limited sample of neurons using an alternative approach to probe this issue. Essentially, we added a second, identical target figure to our standard figure-ground task and rewarded the monkey for making a saccade to the location of either figure. The monkey could thus choose to saccade to either target, as both were rewarded, but the natural preference was to select the target closer to the fixation point (41). By varying the position of the second target, this design allowed us to compare the response to an identical stimulus situated over the neuron's RF when it was or was not the target for a saccade. Although the FGM magnitude was significantly smaller when the figure overlying the RF was not the target for a saccade compared with when it was the saccade target ($P = 0.005$, Wilcoxon matched pairs test; $n = 14$), we nonetheless continued to observe a long latency increase in firing to the figure stimulus overlying the RF, even in this condition (Fig. S2*B*). There was a significant difference ($P < 0.001$, Friedman ANOVA; $n = 14$) in the magnitude of the evoked responses to the different stimulus conditions, and the responses to the figure stimulus for both saccade conditions were significantly larger than those to the ground stimulus ($P < 0.05$, post hoc Wilcoxon tests using Bonferroni correction). Again, these data argue against the interpretation that the effects were wholly dependent on detecting and making a saccade to a target stimulus overlying the RF.

It seems clear that the FGM effect we have observed must contribute to the salience of the figure because it amplifies the strength of the ongoing input from the LGN to the cortex for the figure. Given the magnitude of the effect, it might also index an attentional mechanism driven by feedback (42) (again, however, one that highlights salience), but this will require further examination, as our paradigm could not distinguish between exogenously captured attention directed toward the RF and figure-ground modulation. Studies in V1 have shown separate phases of activity relating to figure-ground separation and a subsequent attentional modulation. These have been timed at ∼60 and ∼140 ms, respectively, using a similar dot motion-defined figure (43). A psychophysical study of the tradeoff between dot speed and presentation time revealed that for human perception, there was a time constant an order of magnitude larger for detecting a figure defined by dot motion as opposed to luminance (44). The median latency we recorded in LGN, 90 ms, is benchmarked by the average saccadic RT of our monkeys (190 ms) and by the latency to motion onset in area V5/MT, which is contingent on dot speed, but estimated (under anesthesia) at 72 ms for our speed of 4°/s (45). Thus, we infer that reentry from V5/MT, via V1, is a plausible mechanism for motion-defined FGM in the LGN, further highlighting the potential for dynamic interplay between stations along the neuraxis of motion processing (7). Indeed, we have recently shown that feedback from V5/MT in the anesthetized monkey is able to influence the responses of LGN neurons to moving stimuli originating from spatial foci substantially beyond their classical RF (30), further underlining its potential role in mediating the motion-defined FGM we report here. Earlier work in anesthetized macaques has also demonstrated the potential contribution of corticogeniculate feedback from V1 to the LGN to extraclassical RF responses (11, 16), further underlining the likely role of feedback mechanisms to these effects. Again, the interesting difference with the current data is the magnitude of the effect we observed here.

Although thalamic relay nuclei have traditionally been regarded as simple sensory relays to the primary sensory cortex, there is a large body of evidence that now suggests cortical feedback connections to the thalamus can influence the transmission of information through it in a functionally selective manner (7, 9, 14). These feedback connections allow for the abstract of the higher-level cortical processes to be fed back into the LGN, with a weighting linked to behavioral salience and attention. Probing these issues to reveal such influences requires a reappraisal of the response characteristics of LGN cells according to their responses to classes of visual stimuli and behavioral tasks more commonly linked to the analysis of higher-level visual function (30, 42). This we have attempted here, and we believe our observations underline the fact that the visual thalamus is essentially embedded in the cortical circuitry and should be seen thus, rather than as forming a distinct input stage serving only to relay

information up the system. These new observations, together with other work in the field (7, 30, 42, 46, 47), also contain the implication that on a moment-by-moment basis, the input to the visual cortex from the thalamus is refined to reflect what the system as a whole (7, 9) considers to be the stimulus engaging its input, rather than simply what the component input channels would indicate in isolation.

Materials and Methods

All procedures were carried out in accordance with the Animals (Scientific Procedures) Act 1986 and were approved by the local ethical committee at University College London Institute of Ophthalmology and by the UK Home Office. Two naive male Macaca mulatta monkeys, each weighing 7–9 kg, were trained, using solely positive reinforcement techniques in accordance with the Prescott review recommendations, to voluntarily enter a Crist Instrument primate chair and were habituated to the laboratory environment. Surgical procedures and extracellular recording methods are described in *SI Materials and Methods*.

Visual Stimulation and Behavioral Tasks. Visual stimuli were generated in Matlab (Mathworks Inc.), using the Psychophysics toolbox running a custom stimulus generator (dx.doi.org/10.5281/zenodo.11080). See *SI Materials and Methods* for further details. Before any recording, animals were trained to the laboratory environment by sitting comfortably under head fixation. Next, animals were trained using fluid reward, in conjunction with fluid control where necessary, to view the monitor binocularly and to maintain fixation for 2–3 s within a 1° radius fixation window around a red fixation spot subtending 0.2° visual angle; eye position was monitored using an Eyelink 1000 infrared eye tracker (SR Research Ltd) recording at 250 Hz. During this fixation period, we presented a range of RF-isolating stimuli (see following) parafoveally; this enabled us to locate and identify RFs of LGN cells for further study during experimental recording sessions. Animals were subsequently trained in the main figure-ground experimental task. Again, stimuli were presented under binocular viewing conditions and animals were trained to initiate fixation within a 1° radius fixation window around a yellow fixation spot presented against a static full-screen random dot display for at least 0.4 s (although in general the monkeys fixated much more precisely on the fixation spot; see Fig. S2*C*). Once the fixation criteria were met, motion was initiated, and both the figure and ground random dot stimuli moved in opposite directions. To complete the task successfully and receive a drop of preferred fruit juice, the animal had to saccade to the location of the figure within 500 ms of stimulus motion onset. Saccades were identified on the basis of their velocity and acceleration.

During recording sessions, before running the figure-ground experimental task, we ran a battery of preliminary tests using a range of RF-isolating stimuli, including a range of contrast, chromatic, and opponent-defined stimuli to determine RF location and physiological response properties (11, 26, 30, 42). We used these RF characterizations (specifically size, opponency and chromaticity, and monocularity), along with stereotypical shifts in eye preference and classical retinotopic progression through penetration depth (48, 49) and the 3D chamber coordinate reconstructions of the MRI, to ensure our sampling was confined to the LGN. Cells were categorized as parvocellular, magnocellular, and koniocellular according to physiological response properties, electrode depth, and stereotypical shifts in eye preference (11, 26, 30, 42). To ensure that one location of the figure stimulus was accurately located over the RF center, the location and extent of the RF was carefully assessed, using a range of stimuli including flashing spots (or bars) of light, drifting bars, and/or edges and patches of sinusoidal grating. In particular, we documented the location and spatial extent of the RF center by exploring the spatial distribution of locations from which a contrast-modulated patch or a patch of drifting grating elicited responses. A variety of patch sizes (0.5–1°) were normally used for this test. They were presented in a randomized sequence over a set of spatial locations defined in rectangular coordinates. The location giving the largest response was used to define the center location, and the coordinates of the spatial locations were adjusted to match. This involved several iterations with variations of patch size and stimulus coordinates to optimize both centering and assessment of spatial extent. We then assessed area-summation using flashing spots, or patches of drifting grating, varying in diameter and presented in a randomized, interleaved manner. A typical example is shown in Fig. S1.

During the figure-ground task, the figure could appear in one of four equidistant positions away from the fixation spot; one of these positions was centered on the RF of the neuron or neurons under study. Figure locations were varied in a randomized interleaved sequence. Apart from opposite direction of motion, the figure and ground random dot stimuli shared identical parameters: dot size subtended 0.1°, dot speed was 4°/s (dots moved 2.29 pixels/frame), dot density was a constant 25 dots/$^{\circ 2}$/s, dot coherence/correlation was 100% (50). All dots were spatially and positionally antialiased (*SI Materials and Methods*). Between every trial, individual dot position was fully randomized so no two trials exhibited the same spatial per dot configuration. Each dot had a luminance chosen randomly on each trial from a uniform grayscale distribution between and inclusive of the darkest (0.02 cd/m^{-2}) and brightest (65 cd/m^{-2}) luminance values generated by the calibrated monitor. Overall mean background luminance was 32.4 cd/m^{-2}. Dots were not limited lifetime (their kill rate was set to 0). Stimulus motion continued from motion onset until the monkey had successfully completed the task by making a saccade to and refixating at the figure center. To ensure we compared figure and ground conditions with identical stimulus parameters, we collected data for both directions of motion of the figure and ground for each location (four positions and two directions resulted in eight trials per block). Animals normally performed 20 repeated blocks. The monkeys performed the task at ∼80% accuracy overall compared with a random response performance expectation of 25% [79.8 ± 1.25% SE ($n = 91$) and 83.4 ± 2.43% SE ($n = 49$) for each monkey, respectively]. Figure size was normally set to 3° or 4° [in accordance with typical sizes used previously in V1 (38)] but was reduced in some cases to 2° or 2.5° to ensure the figure border was at least 1° away from the fixation point. This reduction in figure size did not affect the results; there was no significant correlation between FGM magnitude and stimulus size ($P = 0.430$; $R = -0.067$; Spearman Rank R test).

Data Analysis. Responses were only analyzed for correct trials. For each stimulus condition, responses were compiled into an average response histogram, using a bin width of 10 ms. We used the onset of motion to mark time-zero and computed background activity from a 200-ms time epoch immediately before motion onset. For each cell, we computed the time to saccade initiation on a trial-by-trial basis and restricted our analysis window across all trials to spikes that preceded the earliest saccade initiation time. We defined the average response for each stimulus type as the mean firing rate of the neuron for the period between response onset and this earliest saccade initiation time and calculated evoked responses by subtracting background activity. The response onset latency was defined as the first sampling window after motion onset where the firing rate exceeded background discharge rates by more than the 99% bootstrapped confidence interval (bias corrected and accelerated percentile method; Matlab), provided it was followed immediately by at least two successive bins meeting this criterion. Cells were excluded from further analysis if neither the figure nor ground response, as defined earlier, exceeded the 99% bootstrapped confidence interval of the background activity level. Receptive fields were parafoveal, and all were located within 15° of the fovea, with >90% recorded within the central 10° (median eccentricity, 7.0 ± 2.93° SD; $n = 140$).

For each cell, we calculated a figure versus ground modulation index (FGM), calculated as: $\text{FGM} = 100 * [(R_{\text{figure}} - R_{\text{ground}})/(R_{\text{figure}} + R_{\text{ground}})]$, where R was the evoked response for the given condition. In accordance with previous work in V1 (3, 6, 38), we averaged the responses to both directions of motion before computing the FGM index. Thus, the figure and ground responses resulted from exposing the RF to the identical set of local features across trials (although "ground" trials were three times more frequent), ensuring our results were not influenced by any potential difference in the responses to the two directions of motion [because of the weak direction biases sometimes observed in macaque LGN cells (24)]. We regarded cells that showed an FGM value greater than 20% as showing evidence of figure-to-ground response enhancement.

A potential concern was that a variation in the incidence of microsaccadic eye movements between figure and ground stimulation conditions could lead to a difference in neural responses. To detect microsaccades, we used the velocity-based algorithm code from Engbert and Mergenthaler (51) (see *SI Materials and Methods*). For each unit, we counted the number of microsaccades in the time epoch spanning 200 ms before motion onset (our baseline time period) to the earliest saccade initiation time for both figure and ground stimulus conditions. We expressed the results as a ratio of the number of microsaccades per trial (to compensate for the difference in trial numbers for the two conditions). There was no significant difference ($P = 0.145$, Wilcoxon matched pairs test; $n = 140$) in the incidence of microsaccades between figure and ground stimulation conditions. There was also no significant correlation between FGM magnitude and microsaccade incidence (for either figure or ground stimuli) across our sample ($P = 0.325$, $R = 0.085$; and $P = 0.677$, $R = 0.036$, respectively for figure and ground conditions, Spearman Rank R test).

To construct average population histograms, we first normalized the smoothed (at 1.5 times the bin width) peristimulus time histogram for individual neurons, after subtraction of background firing, to their maximum firing rate. Normalized responses of all neurons were then averaged. For individual data

examples (e.g., Fig. 1), firing rate density functions were constructed by convolving the spike trains with a ±15-ms Gaussian smoothing kernel after exclusion of trials that included microsaccades occurring in the time epoch spanning from 200 ms before figure onset to the end of the analysis time window. Unless otherwise indicated, for population statistics, we used the median as a measure of central tendency and nonparametric two-tailed tests for population data comparisons, as the data were not normally distributed (Shapiro-Wilk normality test).

ACKNOWLEDGMENTS. This work was supported by the Biotechnology and Biological Sciences Research Council Grant G022305/1 and the Medical Research Council Grant G0701535.

1. Grossberg S, Mingolla E (1985) Neural dynamics of form perception: Boundary completion, illusory figures, and neon color spreading. *Psychol Rev* 92(2):173–211.
2. Mumford D, Kosslyn SM, Hillger LA, Herrnstein RJ (1987) Discriminating figure from ground: The role of edge detection and region growing. *Proc Natl Acad Sci USA* 84(20):7354–7358.
3. Lamme VA, Supèr H, Spekreijse H (1998) Feedforward, horizontal, and feedback processing in the visual cortex. *Curr Opin Neurobiol* 8(4):529–535.
4. Marcus DS, Van Essen DC (2002) Scene segmentation and attention in primate cortical areas V1 and V2. *J Neurophysiol* 88(5):2648–2658.
5. Pessoa L, De Weerd P, eds (2003) *Filling in. From perceptual completion to cortical reorganization* (Oxford Univ. Press, New York).
6. Poort J, et al. (2012) The role of attention in figure-ground segregation in areas V1 and V4 of the visual cortex. *Neuron* 75(1):143–156.
7. Sillito AM, Cudeiro J, Jones HE (2006) Always returning: Feedback and sensory processing in visual cortex and thalamus. *Trends Neurosci* 29(6):307–316.
8. Gilbert CD, Sigman M (2007) Brain states: Top-down influences in sensory processing. *Neuron* 54(5):677–696.
9. Briggs F, Usrey WM (2011) Corticogeniculate feedback and visual processing in the primate. *J Physiol* 589(Pt 1):33–40.
10. Sillito AM, Jones HE, Gerstein GL, West DC (1994) Feature-linked synchronization of thalamic relay cell firing induced by feedback from the visual cortex. *Nature* 369(6480):479–482.
11. Jones HE, et al. (2012) Differential feedback modulation of center and surround mechanisms in parvocellular cells in the visual thalamus. *J Neurosci* 32(45): 15946–15951.
12. Gulyás B, Lagae L, Eysel U, Orban GA (1990) Corticofugal feedback influences the responses of geniculate neurons to moving stimuli. *Exp Brain Res* 79(2):441–446.
13. Briggs F, Usrey WM (2009) Parallel processing in the corticogeniculate pathway of the macaque monkey. *Neuron* 62(1):135–146.
14. Suga N, Xiao Z, Ma X, Ji W (2002) Plasticity and corticofugal modulation for hearing in adult animals. *Neuron* 36(1):9–18.
15. McCormick DA, von Krosigk M (1992) Corticothalamic activation modulates thalamic firing through glutamate "metabotropic" receptors. *Proc Natl Acad Sci USA* 89(7): 2774–2778.
16. Marrocco RT, McClurkin JW, Young RA (1982) Modulation of lateral geniculate nucleus cell responsiveness by visual activation of the corticogeniculate pathway. *J Neurosci* 2(2):256–263.
17. Raudies F, Neumann H (2010) A neural model of the temporal dynamics of figure-ground segregation in motion perception. *Neural Netw* 23(2):160–176.
18. Barnes T, Mingolla E (2013) A neural model of visual figure-ground segregation from kinetic occlusion. *Neural Netw* 37:141–164.
19. Hupé JM, et al. (2001) Feedback connections act on the early part of the responses in monkey visual cortex. *J Neurophysiol* 85(1):134–145.
20. Rossi AF, Desimone R, Ungerleider LG (2001) Contextual modulation in primary visual cortex of macaques. *J Neurosci* 21(5):1698–1709.
21. Self MW, van Kerkoerle T, Supèr H, Roelfsema PR (2013) Distinct roles of the cortical layers of area V1 in figure-ground segregation. *Curr Biol* 23(21):2121–2129.
22. Dow BM (1974) Functional classes of cells and their laminar distribution in monkey visual cortex. *J Neurophysiol* 37(5):927–946.
23. Blasdel GG, Fitzpatrick D (1984) Physiological organization of layer 4 in macaque striate cortex. *J Neurosci* 4(3):880–895.
24. Lee BB, Creutzfeldt OD, Elepfandt A (1979) The responses of magno- and parvocellular cells of the monkey's lateral geniculate body to moving stimuli. *Exp Brain Res* 35(3):547–557.
25. Carrasco M (2011) Visual attention: The past 25 years. *Vision Res* 51(13):1484–1525.
26. Wiesel TN, Hubel DH (1966) Spatial and chromatic interactions in the lateral geniculate body of the rhesus monkey. *J Neurophysiol* 29(6):1115–1156.
27. Jones HE, Sillito AM (1991) The length-response properties of cells in the feline dorsal lateral geniculate nucleus. *J Physiol* 444:329–348.
28. Sceniak MP, Chatterjee S, Callaway EM (2006) Visual spatial summation in macaque geniculocortical afferents. *J Neurophysiol* 96(6):3474–3484.
29. Lamme VA (1995) The neurophysiology of figure-ground segregation in primary visual cortex. *J Neurosci* 15(2):1605–1615.
30. Jones HE, et al. (2013) Responses of primate LGN cells to moving stimuli involve a constant background modulation by feedback from area MT. *Neuroscience* 246: 254–264.
31. Allman J, Miezin F, McGuinness E (1985) Stimulus specific responses from beyond the classical receptive field: Neurophysiological mechanisms for local-global comparisons in visual neurons. *Annu Rev Neurosci* 8:407–430.
32. Webb BS, et al. (2002) Feedback from V1 and inhibition from beyond the classical receptive field modulates the responses of neurons in the primate lateral geniculate nucleus. *Vis Neurosci* 19(5):583–592.
33. Solomon SG, White AJR, Martin PR (2002) Extraclassical receptive field properties of parvocellular, magnocellular, and koniocellular cells in the primate lateral geniculate nucleus. *J Neurosci* 22(1):338–349.
34. Cudeiro J, Sillito AM (1996) Spatial frequency tuning of orientation-discontinuity-sensitive corticofugal feedback to the cat lateral geniculate nucleus. *J Physiol* 490(Pt 2):481–492.
35. Allman J, Miezin F, McGuinness E (1985) Direction- and velocity-specific responses from beyond the classical receptive field in the middle temporal visual area (MT). *Perception* 14(2):105–126.
36. Knierim JJ, van Essen DC (1992) Neuronal responses to static texture patterns in area V1 of the alert macaque monkey. *J Neurophysiol* 67(4):961–980.
37. Sillito AM, Grieve KL, Jones HE, Cudeiro J, Davis J (1995) Visual cortical mechanisms detecting focal orientation discontinuities. *Nature* 378(6556):492–496.
38. Zipser K, Lamme VAF, Schiller PH (1996) Contextual modulation in primary visual cortex. *J Neurosci* 16(22):7376–7389.
39. Supèr H, Spekreijse H, Lamme VA (2003) Figure-ground activity in primary visual cortex (V1) of the monkey matches the speed of behavioral response. *Neurosci Lett* 344(2):75–78.
40. Reppas JB, Usrey WM, Reid RC (2002) Saccadic eye movements modulate visual responses in the lateral geniculate nucleus. *Neuron* 35(5):961–974.
41. Carrasco M, Evert DL, Chang I, Katz SM (1995) The eccentricity effect: Target eccentricity affects performance on conjunction searches. *Percept Psychophys* 57(8): 1241–1261.
42. McAlonan K, Cavanaugh J, Wurtz RH (2008) Guarding the gateway to cortex with attention in visual thalamus. *Nature* 456(7220):391–394.
43. Roelfsema PR, Tolboom M, Khayat PS (2007) Different processing phases for features, figures, and selective attention in the primary visual cortex. *Neuron* 56(5):785–792.
44. Regan D, Beverley KI (1984) Figure-ground segregation by motion contrast and by luminance contrast. *J Opt Soc Am A* 1(5):433–442.
45. Lisberger SG, Movshon JA (1999) Visual motion analysis for pursuit eye movements in area MT of macaque monkeys. *J Neurosci* 19(6):2224–2246.
46. O'Connor DH, Fukui MM, Pinsk MA, Kastner S (2002) Attention modulates responses in the human lateral geniculate nucleus. *Nat Neurosci* 5(11):1203–1209.
47. Anderson EJ, Dakin SC, Rees G (2009) Monocular signals in human lateral geniculate nucleus reflect the Craik-Cornsweet-O'Brien effect. *J Vis* 9(12):14.1–18.
48. Malpeli JG, Baker FH (1975) The representation of the visual field in the lateral geniculate nucleus of Macaca mulatta. *J Comp Neurol* 161(4):569–594.
49. Bender DB (1981) Retinotopic organization of macaque pulvinar. *J Neurophysiol* 46(3):672–693.
50. Britten KH, Shadlen MN, Newsome WT, Movshon JA (1992) The analysis of visual motion: A comparison of neuronal and psychophysical performance. *J Neurosci* 12(12):4745–4765.
51. Engbert R, Mergenthaler K (2006) Microsaccades are triggered by low retinal image slip. *Proc Natl Acad Sci USA* 103(18):7192–7197.

Supporting Information

Jones et al. 10.1073/pnas.1405162112

SI Materials and Methods

Surgical Procedures. Surgery was performed using aseptic techniques under full general anesthesia for the implantation of the head post and recording chamber. Anesthesia was induced with a ketamine/medetomidine mixture (6.4 mg/kg ketamine and 0.08 mg/kg medetomidine, i.m.), and i.v. access established after atropine administration (atropine sulfate 0.04 mg/kg i.m.). After intubation, anesthesia was maintained using isoflurane [1–2.5% (vol/vol)] in O_2. Blood pressure, electrocardiogram, end-tidal CO_2, rectal temperature, and peripheral oxygenation were continually monitored. A thermostatically controlled heat blanket was used to main-tain body temperature at 37 °C, and i.v. fluids were given as required. Animals were given s.c. injections of antibiotic (Betamox LA, 0.1 mL/kg) and a nonsteroidal antiinflammatory (Meloxicam 0.2 mg/kg) at the commencement of the surgical procedure and also received oral antibiotic (Synulox palatable drops, 12.5 mg/kg, twice daily) and nonsteroidal antiinflammatory medication (meloxicam 0.1 mg/kg daily) for a minimum period of 5 d pre- and postsurgery. At the end of the surgical procedure, buprenorphine (0.01 mg kg^{-1}, i.m.) was administered for analgesia and repeated twice per day for up to 3 d as needed. Animals were recovered under supervision in protected and warm environments. The implantation of headpost and chamber and the craniotomy were all performed in the same surgical procedure.

We used acrylic-free titanium implants (1) localized stereotaxically after a full structural MRI scan to target the lateral geniculate nucleus. Chambers were custom-angled based on the MRI data to optimize placement on the skull.

Visual Stimulation. Visual stimuli were generated in Matlab (Mathworks Inc.), using the Psychophysics toolbox (2, 3) running a custom stimulus-generator (dx.doi.org/10.5281/zenodo.11080). This enabled high-quality random dot generation; all dots were spatially and positionally antialiased. Floating-point pixel values were used to specify position. This meant subpixel blending minimized artifacts where movement on screen is forced to the nearest integer pixel. Individual "pixels" thus have a more linear response (rounding does not cause them to suddenly light up). The gamma-corrected visual display was an Iiyama HM204DT CRT driven at a resolution of 1280 × 1024 pixels (with each pixel subtending a visual angle of 0.03°) at an 85-Hz vertical refresh rate; we used a DataPixx (VPixx Technologies Inc.) to extend contrast range up to 14 bits when necessary.

Electrophysiological recording. We recorded extracellular activity from LGN neurons using tetrodes (Thomas Recording; impedance range 0.5–0.9 MΩ) driven transdurally by a Thomas minimatrix system micromanipulator (Thomas Recording). The full wideband signal was amplified, high-pass filtered at 0.5 Hz, and stored along with temporally precise strobed words (display-locked with microsecond precision by the DataPixx, indicating stimulus and behavioral conditions) at 40 KHz, using an Omniplex recording system (Plexon Inc). Spike waveforms were then further band-pass-filtered from 250 to 8,000 Hz and thresholded using OfflineSorter software (Plexon Inc). We identified distinct single-unit and multiunit waveform clusters, using manually refined principal component analysis tetrode sorting methods in OfflineSorter. The resultant spike times along with the stimulus and behavioral markers were then analyzed using customized Matlab routines.

Microsaccade detection. To detect microsaccades, we used the velocity-based algorithm code from Engbert and Mergenthaler (4) that defines microsaccades as parts of the eye movement trajectory, where velocity exceeds a relative velocity threshold multiple (λ) of the median SD. We used a relative velocity threshold set to five median-based SDs of the velocity values observed (λ=5), a temporal threshold of two samples (8 ms), and a maximum angular excursion of <1°.

1. Adams DL, Economides JR, Jocson CM, Parker JM, Horton JC (2011) A watertight acrylic-free titanium recording chamber for electrophysiology in behaving monkeys. *J Neurophysiol* 106(3):1581–1590.
2. Brainard DH (1997) The Psychophysics Toolbox. *Spat Vis* 10(4):433–436.
3. Pelli DG (1997) The VideoToolbox software for visual psychophysics: Transforming numbers into movies. *Spat Vis* 10(4):437–442.
4. Engbert R, Mergenthaler K (2006) Microsaccades are triggered by low retinal image slip. *Proc Natl Acad Sci USA* 103(18):7192–7197.

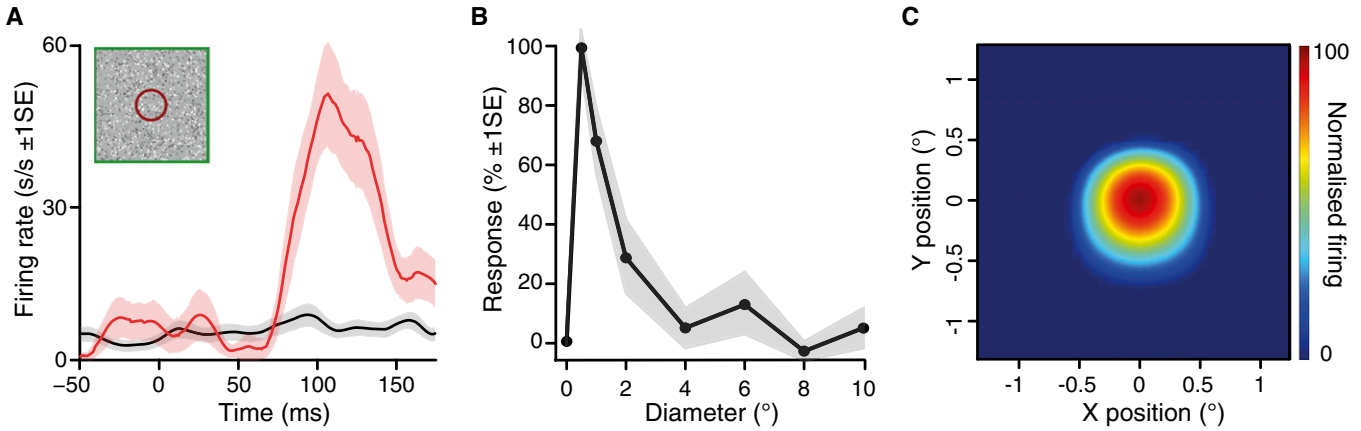

Fig. S1. Example figure-ground response together with the location and spatial extent of the cell's RF center. (*A*) Typical example of enhancement of neuronal firing when the figure, as opposed to the ground component of the stimulus, was located over the RF. SDF to figure (red) and ground (black) stimulus conditions overlying the RF. Time epoch commences 50 ms before stimulus motion onset and ends before saccade initiation. Shading indicates ±1 SE. Inset schematic denotes the size of the RF relative to the size of figure. Figure size 4°. (*B* and *C*) Area summation tuning curve (*B*) and surface map (*C*) documenting the location and extent of the cell's RF. The tuning curve in *B* plots the variation in response magnitude for increasing diameters of a flashed spot of light located over the RF, whereas the surface map in *C* plots the response to a 0.75° flashing spot presented at a range of locations in visual space encompassing the cell's RF locations. For both plots, responses were normalized with respect to the optimal evoked response. Shading in *B* indicates ±1 SE.

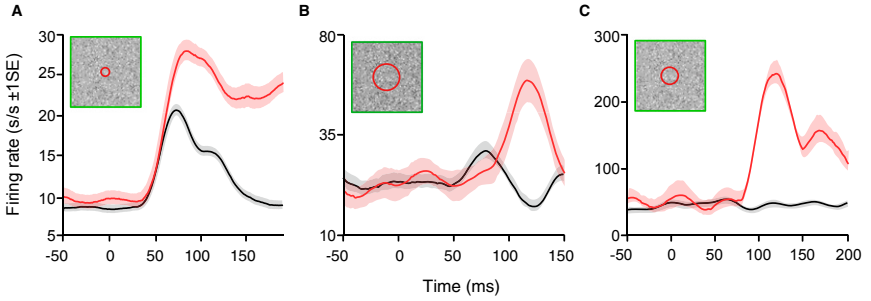

Fig. S2. Enhancement of neuronal firing when the figure, as opposed to the ground component of the stimulus, was located over the RF. (*A*) Response of an example LGN neuron showing an initial early transient response to the stimuli. SDF to figure (red) and ground (black) stimulus conditions (±1 SE) overlying the RF. Time epoch commences 50 ms before stimulus motion onset and ends before saccade initiation. Inset schematic denotes the size of the RF relative to the size of figure. (*B*) Enhancement of neuronal firing to a figure located over the RF, when the figure was not the target for a saccade. Essentially, we added a second, identical target figure to our standard figure-ground task and rewarded the monkey for making a saccade to the location of either figure. The monkey could thus choose to saccade to either target, and this allowed us to record data when the figure located over the RF was not the target for a saccade. Color conventions as in *A*. (*C*) The monkeys fixated much more precisely on the fixation spot than demanded by the experimental fixation window, and robust FGM responses were maintained when we confined the data analysis to those trials where the monkeys maintained fixation within a small region of the fixation window. Example shows the response pattern for trials where fixation was confined within a 0.25° radius fixation window. Other conventions as in *A*.

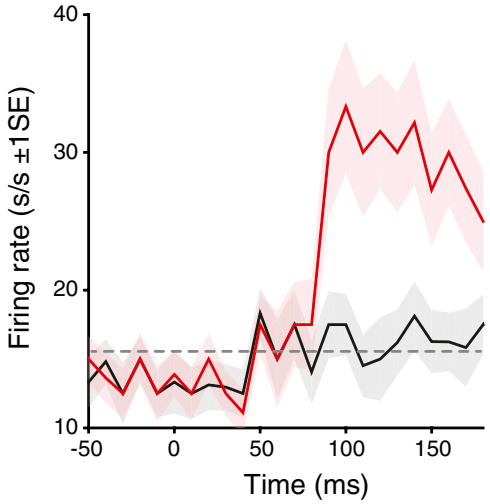

Fig. S3. Averaged population responses to figure (red) and ground (black) stimulus conditions overlying the RF, for our single unit cell sample (n = 77). Shading represents ±1 SE. Motion onset occurred at time 0 ms. Horizontal dotted line denotes background plus 99% confidence limit. In contrast to the average population histograms shown in Figs. 2, 3, and 4, no normalization was applied to the individual data records before averaging.